

Phase structure of lattice QCD with two flavors of Wilson quarks at finite temperature and chemical potential

Liang-Kai Wu*

School of Physics and Engineering, Zhongshan (Sun Yat-Sen) University, Guangzhou 510275, China

Xiang-Qian Luo

CCAST (World Laboratory), P.O. Box 8730, Beijing 100080, China

School of Physics and Engineering, Zhongshan (Sun Yat-Sen) University, Guangzhou 510275, China

He-Sheng Chen

Department of Physical Science and Technology, Yangzhou University, Yangzhou 225009, China

(Dated: December 2, 2024)

We present results for phase structure of lattice QCD with two degenerate flavors ($N_f = 2$) of Wilson quarks at finite temperature T and baryon chemical potential $\mu_B \leq \pi T$. Our simulations are performed at $\kappa = 0, 0.005, 0.165$ with imaginary chemical potential for which the fermion determinant is positive, κ is the hopping parameter. By analytic continuation of the data to real μ , we obtain the transition temperature as a function of μ_B for $\mu_B \lesssim 500\text{MeV}$. We attempt to determine the nature of transition by histogram, MC history, and finite size scaling. In the infinite heavy quark limit, the transition is of first order. At intermediate values of m_q , the MC simulations show absence of phase transition.

PACS numbers: 12.38.Gc, 11.10.Wx, 11.15.Ha, 12.38.Mh

I. INTRODUCTION

QCD at finite temperature and density is of fundamental importance, both on theoretical and phenomenological grounds. It describes relevant features of particle physics in the early universe, in the neutron stars and in the heavy ion collisions. At high density and low temperature, some QCD-inspired models suggest a rich phase structure[1], and at sufficient high temperature and small density, QCD predicts a transition (In this paper “transition” refers to the change in dynamics, irrespective of the order of the phase transition.) from low temperature hadronic matter to high temperature quark gluon plasma (QGP). Probing this transition is one of the main purposes of the experiments of SPS, LHC(CERN) and RHIC(Brookhaven). Because QCD is strongly interacting, perturbative methods do not apply, and the only first principles method to investigate these transitions is by means of lattice Monte Carlo (MC) simulation. However, lattice MC simulation is based on importance sampling, which can not be directly applied to the nonzero baryon density case because of the complex fermion determinant[2] for SU(3) gauge theory.

Enormous efforts have been made to solve this complex action problem. Fodor and Katz[3] used a two-dimensional generalization of the Glasgow reweighting method[4] to study the phase diagram for lattice QCD with Kogut-Susskind (KS) fermions[5]; Allton *et al.*[6] attempted to improve this method by Taylor expansion of the fermionic determinant and observable around $\mu = 0$.

The imaginary chemical potential method[7, 8] has also been employed to circumvent the “sign problem”. D’Elia and Lombardo[8] applied it to investigate the phase diagram of lattice QCD with four flavors of KS fermions. De Forcrand and Philipsen studied the phase diagram of lattice QCD with two flavors [7], three flavors[9] and (2+1) flavors[10] of KS fermions.

Monte Carlo simulation with imaginary μ has a couple of technical advantages. It is computationally simple and allows control over the systematic error by fitting the nonperturbative data to a Taylor series. Furthermore, it is a good testing ground for effective QCD models: analytic results can always be continued to imaginary μ and be compared with the numerics there. The main disadvantage of this approach is its limitation to the range $|\mu|/T < \pi/3$ [7].

The KS fermion and Wilson fermion approach have their own advantages and disadvantages. The KS fermion formalism preserves the chiral symmetry, whereas it does not completely solve the species doubling problem. One staggered flavor at lattice corresponds to four flavors in the continuum limit and in simulation the fermion determinant is replaced by its fourth root. Such a replacement is mathematically unjustified[11], and it might lead to the locality problem in numerical simulations[12]. In Ref. [13], it is pointed out that the fourth root of the staggered fermion determinant has phase ambiguities which become acute when $\text{Re}(\mu)$ exceeds half of the pion mass.

Although Wilson fermions explicitly break the chiral symmetry which is one of the most important symmetries of QCD, they completely solve the species doubling problem. So it is of interest to investigate QCD phase diagram with them. In Ref. [16] the phase diagram of lattice QCD with four flavors ($N_f = 4$) of Wilson fermions

*Corresponding author. Email address: liangkaiwu@yahoo.com.cn

was studied by MC simulations at finite temperature T and imaginary chemical potential $i\mu_I$.

In this paper, we attempt to investigate a case which is more physical than four flavors: lattice QCD with two degenerate flavors of Wilson fermions. In Sec. II, we define the lattice action with imaginary chemical potential and the physical observables we calculate. Our simulation results are presented in Sec. III followed by discussions in Sec. IV.

II. LATTICE FORMULATION WITH IMAGINARY CHEMICAL POTENTIAL

The partition function of the system with N_f degenerate flavors of quarks with chemical potential on lattice is

$$\begin{aligned} Z &= \int [dU][d\bar{\psi}][d\psi] e^{-S_g - S_f} \\ &= \int [dU] (\text{Det}M[U])^{N_f} e^{-S_g}. \end{aligned} \quad (1)$$

where S_g is the Yang-Mills action, and S_f is the quark action with the quark chemical potential μ . Here $\mu = \mu_R + i\mu_I$, $\mu_R, \mu_I \in \mathcal{R}$. For S_g , we use the standard one-plaquette action

$$S_g = -\frac{\beta}{6} \sum_p \text{Tr}(U_p + U_p^\dagger - 2), \quad (2)$$

where $\beta = 6/g^2$, and the plaquette variable U_p is the ordered product of link variables U around an elementary plaquette. For S_f , we use the the Wilson action

$$S_f = \sum_{f=1}^{N_f} \sum_{x,y} \bar{\psi}_f(x) M_{x,y}(U, \kappa, \mu) \psi_f(y), \quad (3)$$

where κ is the hopping parameter, related to the bare quark mass m and lattice spacing a by $\kappa = 1/(2am + 8)$. The fermion matrix is

$$\begin{aligned} M_{x,y}(U, \kappa, \mu) &= \delta_{x,y} - \kappa \sum_{j=1}^3 \left[(1 - \gamma_j) U_j(x) \delta_{x,y-\hat{j}} \right. \\ &\quad \left. + (1 + \gamma_j) U_j^\dagger(x - \hat{j}) \delta_{x,y+\hat{j}} \right] \\ &\quad - \kappa \left[(1 - \gamma_4) e^{a\mu} U_4(x) \delta_{x,y-\hat{4}} \right. \\ &\quad \left. + (1 + \gamma_4) e^{-a\mu} U_4^\dagger(x - \hat{4}) \delta_{x,y+\hat{4}} \right]. \end{aligned} \quad (4)$$

In this paper, we use as our observables the mean value of plaquette which we denote by P , Polyakov loop L and the chiral condensate $\bar{\psi}\psi$, we also calculate their susceptibilities χ .

Polyakov loop L is defined as the followings:

$$\langle L \rangle = \left\langle \frac{1}{V} \sum_{\mathbf{x}} \text{Tr} \left[\prod_{t=1}^{N_t} U_4(\mathbf{x}, t) \right] \right\rangle \quad (5)$$

here and in the following, V is the spatial lattice volume.

The naive definition of chiral condensate $\bar{\psi}\psi$ is not adequate for Wilson quarks because chiral symmetry is explicitly broken by Wilson term, the appropriate chiral condensate $\bar{\psi}\psi$ can be defined via an Ward-Takahashi identity[17], and this properly defined $\bar{\psi}\psi$ was employed in Ref. [18, 19]:

$$\langle \bar{\psi}\psi \rangle = 2m_q a Z \sum_x \langle \pi(x) \pi(0) \rangle \quad (6)$$

where Z is the normalization coefficient, and the tree value of it is $(2\kappa)^2$ which is sufficient for our study. The current quark mass m_q is defined through[17]

$$2m_q \langle 0|P|\pi(\vec{p}=0) \rangle = -m_\pi \langle 0|A_4|\pi(\vec{p}=0) \rangle, \quad (7)$$

where P is the pseudoscalar density $\bar{\psi}\gamma_5\psi$, A_4 is the fourth component of the local axial vector current $\bar{\psi}\gamma_5\gamma_4\psi$, and $|\pi\rangle$ and $|0\rangle$ stand for the pion and vacuum state, respectively. On the lattice,

$$2m_q = m_\pi \lim_{z \gg 1} R(z), \quad (8)$$

with

$$R(z) = -\frac{\langle \sum_{x,y,t} A_z(x,y,z,t) \pi(0) \rangle}{\langle \sum_{x,y,t} \pi(x,y,z,t) \pi(0) \rangle}. \quad (9)$$

The susceptibility of Polyakov loop χ_L is defined as:

$$\chi_L = V \langle (L - \langle L \rangle)^2 \rangle \quad (10)$$

The susceptibility of P and chiral condensate $\bar{\psi}\psi$ are defined as :

$$\chi_P = V N_t \langle (P - \langle P \rangle)^2 \rangle \quad (11)$$

$$\chi_{\bar{\psi}\psi} = V N_t \langle (\bar{\psi}\psi - \langle \bar{\psi}\psi \rangle)^2 \rangle. \quad (12)$$

where N_t is the number of temporal lattice sites. We measure the expectation value of plaquette $\langle P \rangle$, the Polyakov loop norm $\langle |L| \rangle$, the chiral condensate $\langle \bar{\psi}\psi \rangle$ and their susceptibilities χ .

when the system is at crossover or criticality, these physical observable will display sharp changes and the susceptibility will display a peak, from which we determine the transition point. In a finite volume, the susceptibilities are always analytic functions, even in the regime where phase transitions occur. however, in the infinite volume limit, phase transitions reveal themselves through the divergences of the susceptibilities, whereas for crossover, susceptibilities are finite. The order of the transitions can be determined by the finite size scaling of the susceptibilities. The susceptibility at transition

point χ_{max} behaves as $\chi_{max} \propto V^\alpha$, with α the critical exponent. If $\alpha = 0$, the transition is just a crossover; If $0 < \alpha < 1$, it is a second order phase transition; If $\alpha = 1$, it is a first order phase transition, accompanying the double peak structure in the histogram of the quantity O and flip-flops between the two states in the MC history[20].

III. MC SIMULATION RESULTS

In this section, we will present our results for simulating QCD with two degenerate flavors of Wilson fermions at finite temperature T and imaginary chemical potential $i\mu_I$. The HMC algorithm is used[24]. To determine the pseudo-transition point $\beta_c(a\mu_I)$, we use the Ferrenberg-Swendsen reweighting method[21]. The simulations are performed on the $V \times N_t = 8^3 \times 4$ lattice at $\kappa = 0, 0.005, 0.165$. $\delta\tau$ is chosen in such a way that the acceptance rate is approximately 80 – 90% otherwise stated. There are 20 molecular steps with for each trajectory. We generate 20,000 trajectories after 5,000 trajectories for warmup. Ten or twenty trajectories are carried out between measurements. To determine the order of phase transition at some parameters, larger lattices are also used for finite size scaling. When calculating the quark mass m_q , we perform simulations on the $8^2 \times 20 \times 4$ lattice while keeping other parameters unchanged. We use the conjugate gradient method to evaluate the fermion matrix inversion.

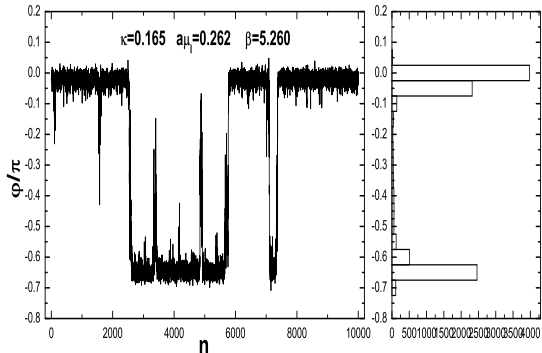


FIG. 1: Histogram of φ/π at RW transition point $a\mu_I = \pi/12 \approx 0.262$, where φ is the Polyakov loop phase.

A. RW TRANSITION AT IMAGINARY CHEMICAL POTENTIAL

In this section, we present the results of simulation for addressing the $Z(3)$ transition, and the simulation is

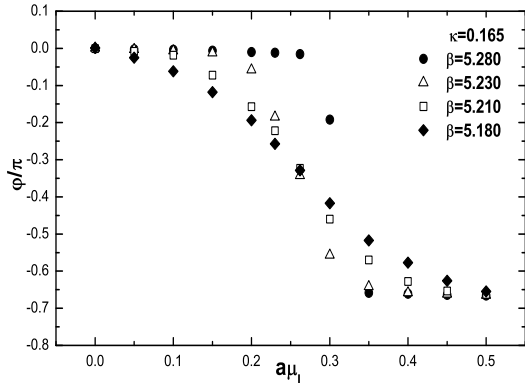


FIG. 2: $\langle\varphi\rangle/\pi$ as a function of $a\mu_I$ for some different values of β .

performed with $\delta\tau = 0.02$ for which the acceptance rate is approximately 90 – 95%.

Lattice $SU(3)$ gauge theory with fermions at imaginary μ has unphysical periodicity with period $2\pi T/N_c$ [7, 8, 27], which limits the validity of the method up to $\mu_I/T = \pi/N_c$. In our case, i.e., $N_c = 3$ and $N_t = 4$, the first Roberge-Weiss (RW) transition to different $Z(3)$ sectors should appear at $a\mu_I = \pi/12 \approx 0.262$. In the high temperature deconfined phase, there is a first order phase transition between different $Z(3)$ sectors, while in the low temperature phase, the transition becomes a crossover at some critical imaginary chemical potential values μ_I^c [7, 8, 27].

$$\frac{\mu_I^c}{T} = \frac{2\pi}{N_c} \left(k + \frac{1}{2} \right). \quad (13)$$

The different $Z(3)$ sectors can be distinguished from each other by the phase of Polyakov loop.

Figure 1 shows the history and probability distribution of the phase φ of the Polyakov loop at $a\mu_I = 0.262$, $\kappa = 0.165$ and $\beta = 5.260$. Figure 2 shows φ/π as a function of $a\mu_I$ at some different values of β . These indicate that at $a\mu_I \approx 0.262$, and $T > T_E$ (where β is larger than [5.245, 5.255]), there is a first order phase transition with $\langle\varphi\rangle$ changing between values of 0 and $-2\pi/3$.

B. DECONFINEMENT TRANSITION AT IMAGINARY CHEMICAL POTENTIAL

In order to investigate the deconfinement transition, we perform measurements of plaquette P , Polyakov loop norm $|L|$, chiral condensate $\bar{\psi}\psi$ and their susceptibility $\chi_P, \chi_{|L|}, \chi_{\bar{\psi}\psi}$ in the first $Z(3)$ sector $a\mu_I < (\pi/3N_t)$ at $\kappa = 0.165$ by using Ferrenberg-Swendsen reweighting method. The values of β at which we make simulation for Ferrenberg-Swendsen reweighting method and the quark

and meson π , ρ screening mass are presented in Table. I except for $a\mu_I = 0.10, 0.18$. In order to calculate the chiral condensate, we must know the quark mass first. At $a\mu_I = 0.10, 0.18$, the values of β at which we mke simulation are the same as those at $a\mu_I = 0.0$ and we use the quark masses at the four different values of β at $a\mu_I = 0.0$ and $a\mu_I = 0.21$ as those values at $a\mu_I = 0.10$ and $a\mu_I = 0.18$, respectively. For the quark mass differs slightly at the same β and different $a\mu_I$. The value of plaquette, Polyakov loop norm, chiral condensate and their susceptibilities are plotted in Fig. 3 and Fig. 4, respectively (we only plot them for three values of $a\mu_I$).

From Fig. 3, one sees that around some β 's, the values of P , $|L|$ and chiral condensate change rapidly. Fig. 4 tells that the location of the peaks for χ_P , χ_L , $\chi_{\bar{\psi}\psi}$ are consistent within errors. We determine the transition point $\beta_c(a\mu_I)$ from the location of susceptibility peaks, the results are listed in Table. II. In Ref. [7], it has been generally argued that the pseudo-critical transition line $\beta_c(a\mu_I)$ is an even function of $a\mu_I$ and can be fitted well by a polynomial of degree one in $(a\mu_I)^2$ without taking into account the term of degree two in $(a\mu_I)^2$, that is to say:

$$\beta_c(a\mu_I) = c_0 + c_1(a\mu_I)^2 + O(a^4\mu_I^4), \quad (14)$$

We use the least squares method to fit the data in Table II, the coefficients and χ^2/dof are listed in Table III,

From Table III, we can find that the fitting result from chiral condensate is better than the result from P and L , so it is our choice for the pseudo-critical transition line, the fitting range and the line are presented in Fig. 5.

$$\beta_c(a\mu_I) = 5.202(3) + 0.730(72)(a\mu_I)^2 + O(a^4\mu_I^4). \quad (15)$$

the errors are the fit errors.

C. DECONFINEMENT TRANSITION AT REAL CHEMICAL POTENTIAL μ

Now it is trivial to get the pseudo critical line on the (μ, T) plane with quark mass dependence neglected. Because $\beta_c(a\mu_I)$ is an analytic function of $a\mu_I$ [7], we can analytically continue from imaginary chemical potential to real one. Replacing μ_I by $-i\mu$ in Eq. (15), we obtain $\beta_c(a\mu)$,

$$\begin{aligned} \beta_c(a\mu) &= c_0 - c_1(a\mu)^2 + O(a^4\mu^4) \\ &= 5.202(3) - 0.730(72)(a\mu)^2 + O(a^4\mu^4). \end{aligned} \quad (16)$$

To translate our result into physical unit, we use the two loop perturbative solution to the renormalization group equation between the lattice spacing a and β :

$$a\Lambda_L = \exp \left[-\frac{4\pi^2}{33-2N_f}\beta + \frac{459-57N_f}{(33-2N_f)^2} \ln \left(\frac{8\pi^2}{33-2N_f}\beta \right) \right]. \quad (17)$$

From this and $T = 1/(aN_t)$, we obtain

$$\frac{T_c(\mu)}{T_c(0)} = \frac{a(\beta_c(0))\Lambda_L}{a(\beta_c(\mu))\Lambda_L} \quad (18)$$

by replacing a with $1/(N_t T_c)$, it gives:

$$\frac{T_c(\mu)}{T_c(0)} = \frac{\exp \left[-\frac{4\pi^2}{33-2N_f}c_0 + \frac{459-57N_f}{(33-2N_f)^2} \ln \left(\frac{8\pi^2}{33-2N_f}c_0 \right) \right]}{\exp \left[-\frac{4\pi^2}{33-2N_f}(c_0 - c_1\frac{\mu}{N_t T_c}) + \frac{459-57N_f}{(33-2N_f)^2} \ln \left(\frac{8\pi^2}{33-2N_f}(c_0 - c_1\frac{\mu}{N_t T_c}) \right) \right]}. \quad (19)$$

Expand the right hand side of Eq. (19) as a series of μ^2 and neglect the terms of higher order, we can obtain the expression of T_c as a function of μ^2 . $a(\beta_c(0))$ is set by the critical temperature for 2-flavor QCD at $\mu_B = 0$.

Recently, Bernard et al.[28] studied the transition temperature of 3-flavor, (2+1) flavor QCD, they obtained $T_c = 169(12)(4)\text{MeV}$ or $T_c = 174(11)(4)\text{MeV}$ for (2+1) flavor. Cheng et al.[29] performed calculation of the transition temperature of (2+1) flavor QCD, and $T_c =$

192(7)(4)MeV is their result. Karsch, Laermann and Peikert obtained $T_c(\mu = 0) = 173(8)\text{MeV}$ in the chiral limit for staggered fermions[30]. Ali Khan et al. used a renormalization group improved gauge action and clover-improved Wilson quark action to investigate 2-flavor QCD and they obtained $T_c(\mu = 0) = 171(4)\text{MeV}$ [18]. The result of Karsch et al. and Ali Khan et al. are consistent with each other. We take 173(8)MeV as $T_c(\mu_B = 0)$,

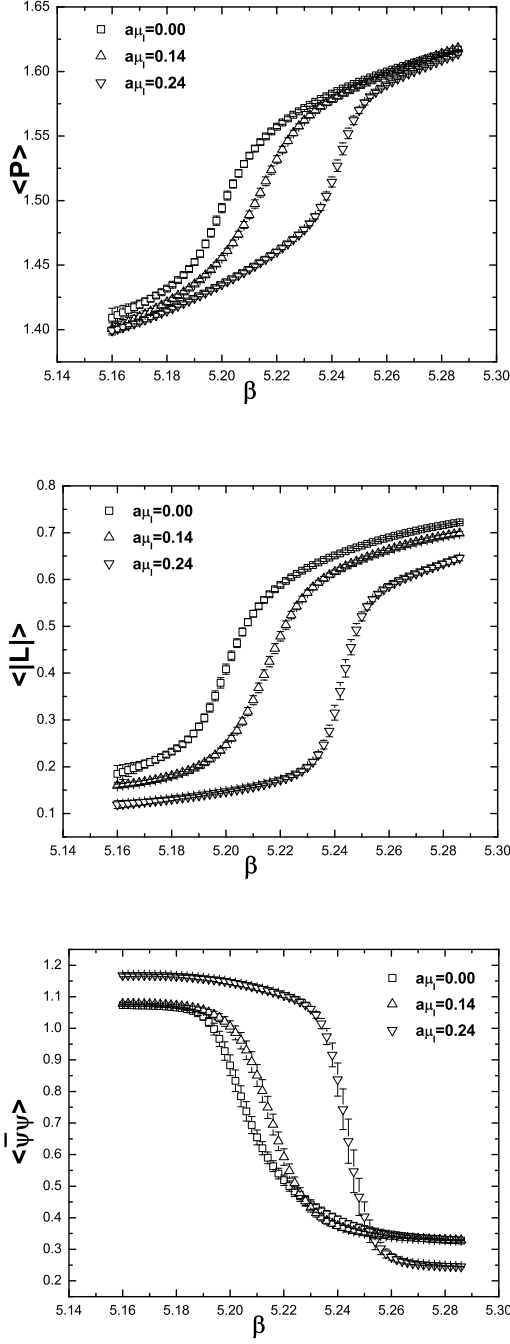


FIG. 3: Mean value of the plaquette, the Polyakov loop norm and the chiral condensate at $\kappa = 0.165$.

therefore the transition line for $N_f = 2$ is described by

$$\frac{T_c(\mu_B)}{T_c(\mu_B = 0)} = 1 - 0.00730(72)\left(\frac{\mu_B}{T}\right)^2, \quad (20)$$

where the baryon chemical potential μ_B is related to the quark chemical potential by $\mu = \mu_B/N_c$ and the error only reflects the error on c_1 . We plot the $T_c(\mu_B)$ function

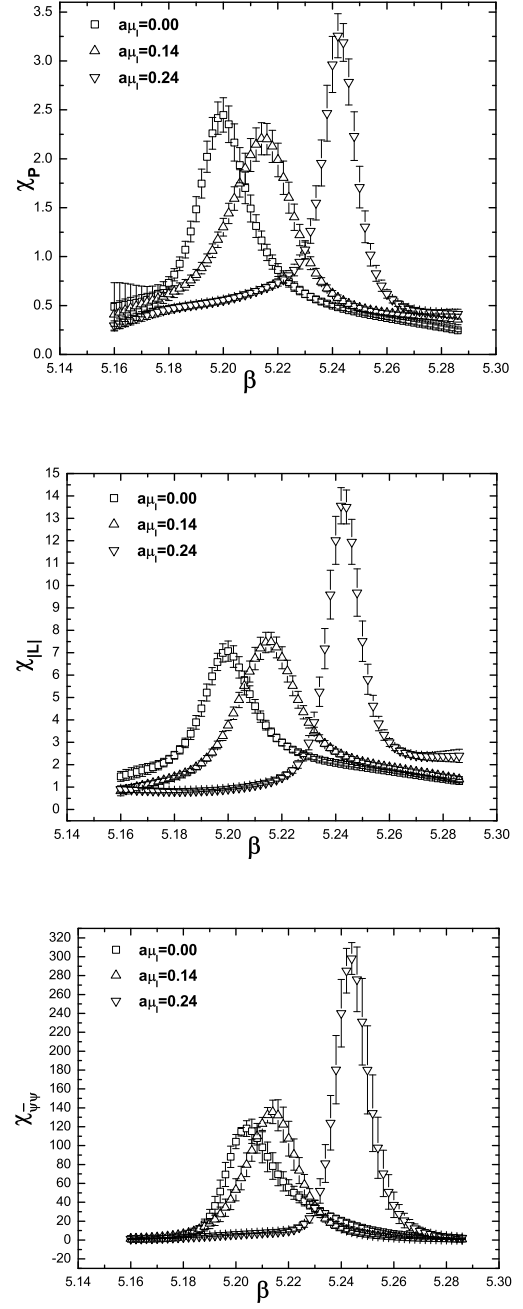


FIG. 4: Susceptibilities for the plaquette, the Polyakov loop norm and the chiral condensate at $\kappa = 0.165$.

in Fig. 6 from which we can see that T_c decreases with increasing μ_B . Because the imaginary chemical potential method is valid in the range $\mu_B/T \leq \pi$, we can obtain the approximate range of $\mu_B \lesssim 500\text{MeV}$ by using the temperature 173MeV or 171MeV at $\mu_B = 0$

TABLE I: Results of π , ρ meson and twice quark screening mass for $N_f = 2$ on $8^2 \times 20 \times 4$ lattice. The acceptance rates are approximately 75 – 83%, with the exception at $a\mu_I = 0.24$, $\beta = 5.24$, at that point, the acceptance rate is 70%.

$a\mu_I$	β	$m_\pi a$	$2m_q a$	$m_\rho a$
0.0	5.195	1.244(2)	0.4193(9)	1.354(2)
	5.215	1.301(2)	0.2550(5)	1.410(1)
	5.235	1.327(2)	0.1893(4)	1.437(1)
	5.255	1.354(2)	0.1386(2)	1.455(1)
0.14	5.195	1.203(2)	0.4542(9)	1.298(2)
	5.215	1.217(2)	0.3286(7)	1.290(2)
	5.235	1.301(2)	0.2024(3)	1.328(2)
	5.255	1.320(2)	0.1546(2)	1.345(2)
0.210	5.195	1.182(3)	0.461(1)	1.274(2)
	5.215	1.140(2)	0.421(1)	1.228(2)
	5.235	1.177(3)	0.2527(7)	1.201(2)
	5.255	1.278(2)	0.1558(3)	1.237(2)
0.240	5.200	1.169(2)	0.456(1)	1.263(2)
	5.220	1.117(3)	0.416(1)	1.211(2)
	5.240	1.098(3)	0.336(1)	1.148(3)
	5.260	1.242(3)	0.1013(2)	1.192(2)

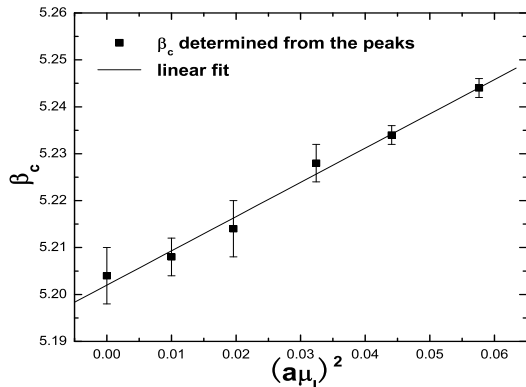


FIG. 5: Location of pseudo critical coupling determined from $\chi_{\bar{\psi}\psi}$, the line shows the fit.

D. THE NATURE OF PHASE TRANSITION

In order to determine the nature of the phase transition, we investigate the history, histogram and finite size scaling of MC simulation at $\kappa = 0, 0.005, 0.165$. On lattice $8^3 \times 4, 12^3 \times 4, 16^3 \times 4$, at $\kappa = 0$ which corresponds to quenched limit or pure gauge theory, we find the critical β is 5.70 by determining the location of the peak of $\chi_{|L|}$. The value of β_c is accurately consistent with the result of Ref. [31]. we plot the history and histogram of $\langle |L| \rangle$

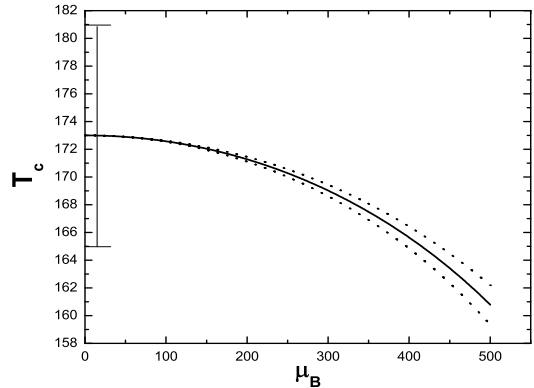


FIG. 6: Transition temperature as a function of μ_B . The dotted lines reflect the error on c_1 , the error bar is due to the uncertainty in $T_c(0)$.

at critical $\beta_c = 5.70$ in Fig. 7. From the histogram and MC history of $\langle |L| \rangle$, we see that near $\beta = 5.70$, there are two-state signals in the system, which are an indication of first order phase transition.

because when $\kappa = 0.0$, quarks have no effect on the system, it is natural that the value of critical β and the two-state signal are the same for other values of $a\mu_I$ in the quenched limit. So we conclude that at other values of $a\mu_I$ in the quenched limit, the phase transition is first order. we also make simulation at $\kappa = 0.005$ on lattice $8^3 \times 4$, the result is presented in Fig. 8 which tell us that for very heavy quarks, the system has the feature of first order transition.

In order to estimate the lattice spacing at $\beta = 5.70$, we use the results in Ref. [32] from which we know that at $\beta = 6.25$, the lattice spacing a on lattice $12^3 \times 36$ in the quenched approximation is $0.505(9)\text{GeV}^{-1}$. We use Eq. (17) with $N_f = 0$ to estimate that lattice spacing $a = 0.938(17)\text{GeV}^{-1}$ at $\beta = 5.70$.

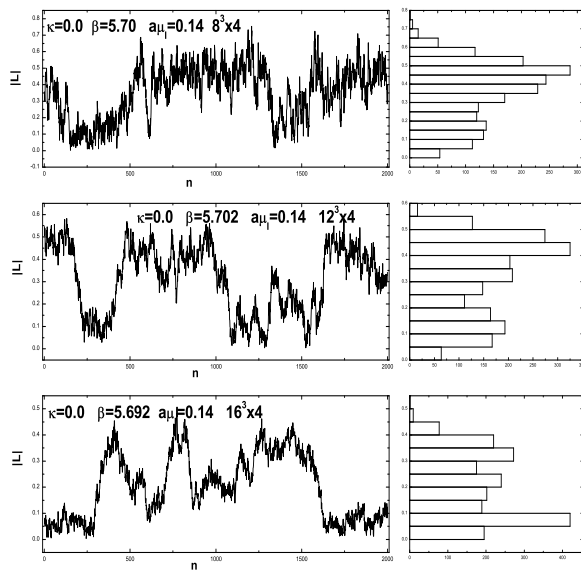
At $\kappa = 0.165, a\mu_I = 0.24$, we evaluate the spatial dependence of susceptibility of Polyakov loop norm, chiral condensate and their time history and histogram on lattice $8^3 \times 4, 10^3 \times 4, 12^3 \times 4, 14^3 \times 4, 16^3 \times 4, 20^3 \times 4$ with acceptance rate 82%, 81%, 75%, 68%, 67%, 51%. At $\kappa = 0.165, a\mu_I = 0.24, \beta = 5.244$ the twice quark mass is $2m_q a = 0.2297(6)$, the acceptance rate is 75%. We present the spatial dependence in Fig. 9, 11 and the time history and histogram on lattice $8^3 \times 4, 12^3 \times 4, 16^3 \times 4$ and $20^3 \times 4$ in Fig. 10, 12. From Fig. 9 we find that the peak heights of Polyakov loop norm susceptibility are approximately the same except for spatial volume 12^3 . The history and histogram of Polyakov loop norm plotted in Fig. 10, together with the peak height change with spatial volume, shows the absence of phase transition. The spatial dependence of chiral condensate susceptibility in Fig. 11 is consistent with a linear behavior in volume, which is expected for a first order phase transi-

TABLE II: Collection of pseudo critical transition points at $\kappa = 0.165$, determined by locating the peak of the susceptibilities.

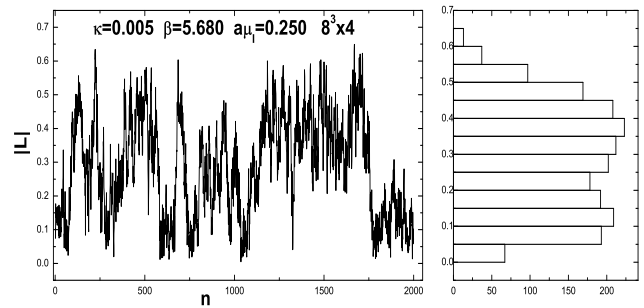
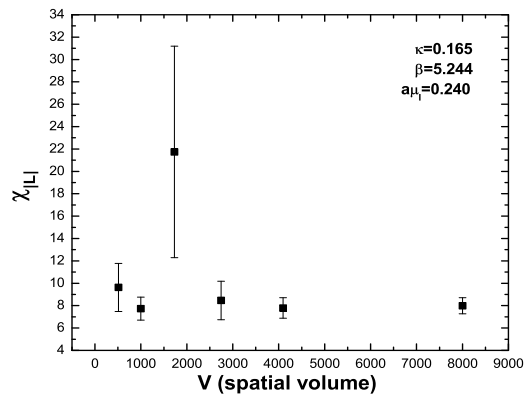
$a\mu_I$	0.00	0.10	0.14	0.18	0.21	0.24
β_C from χ_P	5.200(4)	5.208(4)	5.214(6)	5.226(4)	5.232(4)	5.242(2)
β_C from χ_L	5.200(4)	5.208(4)	5.216(6)	5.226(4)	5.234(2)	5.242(4)
β_C from $\chi_{\bar{\psi}\psi}$	5.204(6)	5.208(4)	5.214(6)	5.228(4)	5.234(2)	5.244(2)

TABLE III: Coefficients of Eq. (14) by fitting the data in Table. II

	c_0	c_1	χ^2/dof
β_C from χ_P	5.201(3)	0.721(63)	0.078
β_C from χ_L	5.201(3)	0.745(75)	0.084
β_C from $\chi_{\bar{\psi}\psi}$	5.202(3)	0.730(72)	0.18

FIG. 7: Time history and histogram of Polyakov loop at $\kappa = 0.0$.

tion. However, we must be cautious to draw a conclusion only from Fig. 11. when we examine the time history and histogram of chiral condensate in Fig. 12, there is no flip-flop behavior between two different values of chiral condensate at all. This similar behavior is also observed for KS fermions in Ref. [33]. So we conclude that the transition at $\kappa = 0.165$, $a\mu_I = 0.24$ is a crossover.

FIG. 8: Time history and histogram of Polyakov loop norm at $\kappa = 0.005$.FIG. 9: Peak height of susceptibility of Polyakov loop norm as a function of spatial volume at $a\mu_I = 0.24$.

IV. DISCUSSION

We have studied the phase diagram of lattice QCD with the two flavor of Wilson fermions through the simulations with imaginary chemical potential. In this case the partition function is periodic in imaginary chemical potential. The different $Z(3)$ sectors are characterized by the phase of Polyakov loop. The $Z(3)$ transition which occurs at $\mu_I/T = 2\pi(k + 1/2)/3$ is of first order in the high temperature phase.

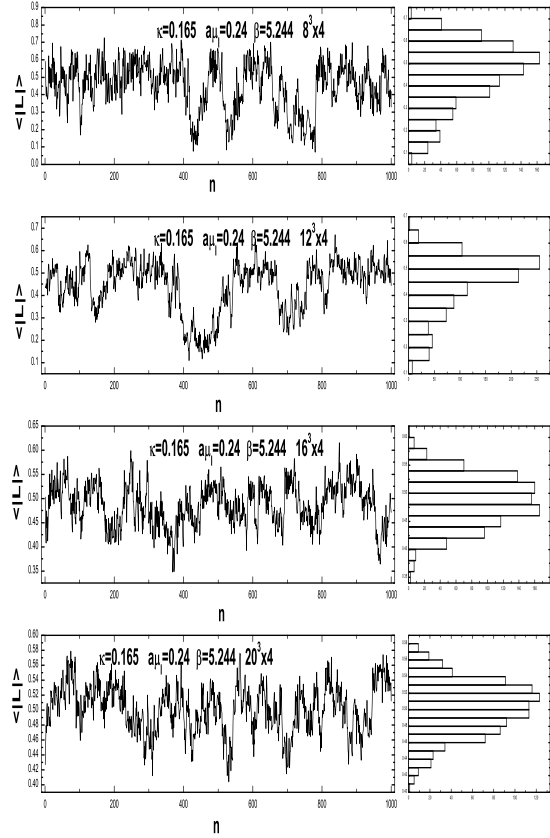


FIG. 10: History and histogram of Polyakov loop norm at different spatial volume at $a\mu_I = 0.24$.

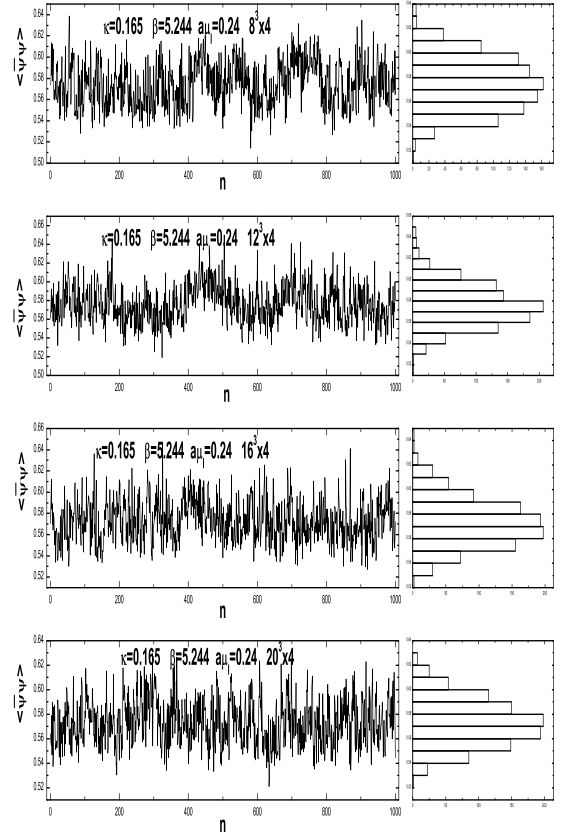


FIG. 12: History and histogram of chiral condensate at different spatial volume at $a\mu_I = 0.24$.

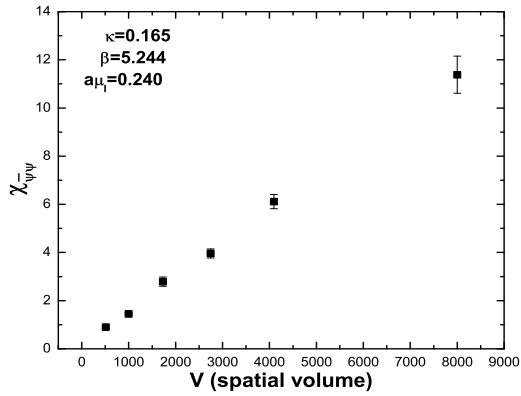


FIG. 11: Peak height of susceptibility of chiral condensate at different spatial volume at $a\mu_I = 0.24$.

Our study shows that there is a first order phase transition at small κ or for heavy quarks. At $\kappa = 0$ which corresponds to infinite heavy quark or quenched limit, it is natural that the β_c and hence the critical temperature has no dependence on the chemical potential based on the fact that the fermions have no effect on the system in quenched limit.

As for the chiral transition, as discussed in Ref. [7], the critical line can be described well by a linear function of μ_B^2 . We make simulation at $\kappa = 0.165$ and obtain the critical line in the chiral limit by neglecting the quark mass dependence. Our central result is represented by Eq. (20) which is qualitatively consistent with yet quantitatively slightly different from that in Ref. [7] taking errors into account. We think that it is probably because our simulation is at a point of quark mass larger than that in Ref. [7]. Solving Eq. (20), we can obtain the $T(\mu_B)$ as a function of μ_B . We plot the chiral transition temperature (MeV) versus baryon chemical potential (MeV) in Fig. 6 from which we find that the chiral transition tem-

perature T_c decreases slowly with increasing μ_B in the range of $\mu_B \lesssim 500\text{MeV}$. This behavior is in accordance with the physical picture. With baryon density increasing, the interaction between quarks and gluons becomes weaker and thus quark and gluon degrees of freedom get more easily excited, therefore, the critical temperature decreases with increasing baryon chemical potential.

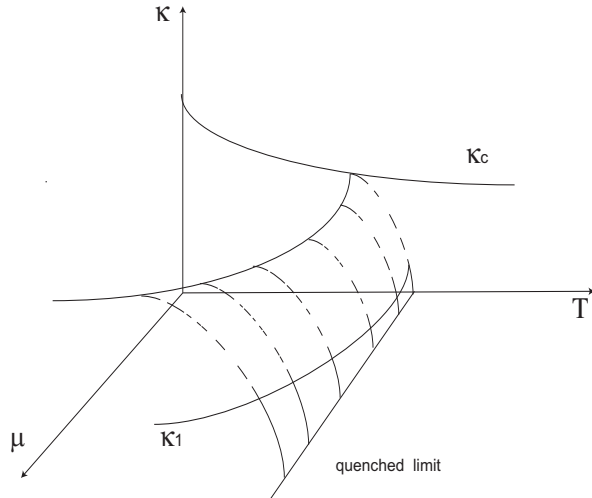


FIG. 13: Expected phase diagram of lattice QCD with two flavors of Wilson fermions in the range of $0 \leq \mu_B \lesssim 500\text{MeV}$. In the chiral limit, the phase transition is assumed to be second order; For $\kappa_1 < \kappa < \kappa_c$, the transition is crossover; for $0 \leq \kappa < \kappa_1$, the transition is first order; for $\kappa = \kappa_1$, the transition is of second order.

From the experience and literature, we expect that in general, the lighter the quark mass, the stronger effect of dynamical fermions appears. At $\kappa = 0.165$, we observe that the chiral condensate changes rapidly around β_c and transition points determined from the susceptibilities of plaquette variable, the Polyakov loop and chiral condensate coincide within errors. The transition at in-

termediate quark mass is a crossover, as discussed in the preceding section.

However, in the chiral limit, theoretical arguments based on QCD-inspired models[22, 23] suggest that the phase transition from the hadronic matter to QGP is of second order for $N_f = 2$. Karsch and Laermann[14, 15] investigate the nature of two flavor QCD transition and their results are consistent with the prediction of a second order; Lattice simulation with Wilson fermions in the chiral limit[25] suggests that the transition be second order; recent simulation of χQCD in the chiral limit[26] suggests that the transition be of second order. We assume that this is the case and present the diagram of two-flavor QCD with $\mu_B \leq 500\text{MeV}$ which is plotted in Fig. 13.

Fig. 13 is the expected phase diagram of lattice QCD with two flavor of Wilson fermions for $\mu_B \lesssim 500\text{MeV}$ in the (μ, T, κ) parameter space. Above the surface $\kappa = \kappa_c$, there is no phase transition. The real physics is below the surface: at each κ corresponding to some quark mass, there is a transition line on the (μ, T) plane. When $\kappa \in [0, \kappa_1)$, corresponding to the heavy quark case, the transition is of first order; When $\kappa = \kappa_1$, the transition is of second order; At the intermediate quark mass, $\kappa \in (\kappa_1, \kappa_c)$, the transition is a crossover; In the chiral limit, $\kappa = \kappa_c$ we assume that the transition is of second order.

Acknowledgments

Liangkai Wu is indebted to Philippe de Forcrand for his valuable helps. We thank the referee very much for the comments. This work is supported by the NSF Key Project (10235040), CAS (KJXC2-SW-N10), Ministry of Education (105135), Guangdong NSF(05101821), and ZARC (06P1). We modify the MILC collaboration's public code[34] to simulate the theory at imaginary chemical potential. The computations are performed on our AMD-Opteron cluster.

-
- [1] M. G. Alford, K. Rajagopal and F. Wilczek, Phys. Lett. B **422**, 247 (1998); R. Rapp, T. Schafer, E. V. Shuryak and M. Velkovsky, Phys. Rev. Lett. **81**, 53 (1998).
 - [2] P. Hasenfratz and F. Karsch, Phys. Lett. B **125**, 308 (1983).
 - [3] Z. Fodor and S. D. Katz, Phys. Lett. B **534**, 87 (2002).
 - [4] I. M. Barbour, S. E. Morrison, *et al.*, Nucl. Phys. A (Proc. Suppl.) **60**, 220 (1998).
 - [5] Z. Fodor and S. D. Katz, JHEP **0203**, 014 (2002).
 - [6] C. R. Allton *et al.*, Phys. Rev. D **66**, 074507 (2002) [arXiv:hep-lat/0204010].
 - [7] P. de Forcrand and O. Philipsen, Nucl. Phys. B **642**, 290 (2002).
 - [8] M. D'Elia and M. P. Lombardo, Phys. Rev. D **67**, 014505 (2003).
 - [9] P. de Forcrand and O. Philipsen, Nucl. Phys. B **673**, 170 (2003).
 - [10] P. de Forcrand and O. Philipsen, JHEP **0701**, 077 (2007) [arXiv:hep-lat/0607017].
 - [11] H. Neuberger, Phys. Rev. D **70**, 097504 (2004).
 - [12] B. Bunk, M. Della Morte, K. Jansen and F. Knechtli, Nucl. Phys. B **697**, 343 (2004).
 - [13] M. Golterman, Y. Shamir and B. Svetitsky, Phys. Rev. D **74**, 071501(R) (2006).
 - [14] F. Karsch and E. Laermann, Phys. Rev. D **50**, 6954 (1994) [arXiv:hep-lat/9406008].
 - [15] F. Karsch, Phys. Rev. D **49**, 3791 (1994) [arXiv:hep-lat/9309022].
 - [16] H. S. Chen and X. Q. Luo, Phys. Rev. D **72**, 034504 (2005).

- [17] M. Bochicchio, L. Maiani, G. Martinelli, G. C. Rossi and M. Testa, Nucl. Phys. B **262**, 331 (1985).
- [18] A. Ali Khan *et al.* [CP-PACS Collaboration], Phys. Rev. D **63**, 034502 (2001) [arXiv:hep-lat/0008011].
- [19] Y. Iwasaki, K. Kanaya, S. Kaya and T. Yoshie, Phys. Rev. Lett. **78**, 179 (1997) [arXiv:hep-lat/9609022].
- [20] M.N. Barber, in *Phase Transitions and Critical Phenomena*, eds. C. Domb and J.L. Lebowitz (Academic Press, New York, 1983), Vol 8.
- [21] A. M. Ferrenberg and R. H. Swendsen, Phys. Rev. Lett. **63**, 1195 (1989).
- [22] R. D. Pisarski and F. Wilczek, Phys. Rev. D **29**, 338 (1984); F. Wilczek, Int. J. Mod. Phys. A **7**, 3911 (1992) [Erratum-ibid. A **7**, 6951 (1992)]; K. Rajagopal and F. Wilczek, Nucl. Phys. B **399**, 395 (1993).
- [23] K. Rajagopal, Nucl. Phys. A **661**, 150 (1999), and refs. therein.
- [24] S. Gottlieb, W. Liu, D. Toussaint, R. L. Renken and R. L. Sugar, Phys. Rev. D **35**, 3972 (1987).
- [25] Y. Iwasaki, K. Kanaya, S. Sakai and T. Yoshie, Z. Phys. C **71**, 337 (1996); Y. Iwasaki, K. Kanaya, S. Kaya, S. Sakai and T. Yoshie, Phys. Rev. D **54**, 7010 (1996).
- [26] J. B. Kogut and D. K. Sinclair, Phys. Rev. D **73**, 074512 (2006).
- [27] A. Roberge and N. Weiss, Nucl. Phys. B **275**, 734 (1986).
- [28] C. Bernard *et al.* [MILC Collaboration], Phys. Rev. D **71**, 034504 (2005) [arXiv:hep-lat/0405029].
- [29] M. Cheng *et al.*, Phys. Rev. D **74**, 054507 (2006) [arXiv:hep-lat/0608013].
- [30] F. Karsch, E. Laermann and A. Peikert, Nucl. Phys. B **605**, 579 (2001),
- [31] F. R. Brown, N. H. Christ, Y. F. Deng, M. S. Gao and T. J. Woch, Phys. Rev. Lett. **61** (1988) 2058.
- [32] Z. H. Mei, X. Q. Luo and E. B. Gregory, Chin. Phys. Lett. **19**, 636 (2002) [arXiv:hep-lat/0202012].
- [33] S. Aoki *et al.* [JLQCD Collaboration], Phys. Rev. D **57**, 3910 (1998) [arXiv:hep-lat/9710048].
- [34] <http://physics.utah.edu/~detar/milc/>